INTERNATIONAL JOURNAL OF
NUMERICAL ANALYSIS AND MODELING
Volume 20, Number 5, Pages 724–738

doi: 10.4208/ijnam2023-1032

A NOVEL DEEP NEURAL NETWORK ALGORITHM FOR THE HELMHOLTZ SCATTERING PROBLEM IN THE UNBOUNDED DOMAIN

ANDY L YANG†

Abstract. In this paper, we develop a novel meshless, ray-based deep neural network algorithm for solving the high-frequency Helmholtz scattering problem in the unbounded domain. While our recent work [44] designed a deep neural network method for solving the Helmholtz equation over finite bounded domains, this paper deals with the more general and difficult case of unbounded regions. By using the perfectly matched layer method, the original mathematical model in the unbounded domain is transformed into a new format of second-order system in a finite bounded domain with simple homogeneous Dirichlet boundary conditions. Compared with the Helmholtz equation in the bounded domain, the new system is equipped with variable coefficients. Then, a deep neural network algorithm is designed for the new system, where the rays in various random directions are used as the basis of the numerical solution. Various numerical examples have been carried out to demonstrate the accuracy and efficiency of the proposed numerical method. The proposed method has the advantage of easy implementation and meshless while maintaining high accuracy. *To the best of the author's knowledge, this is the first deep neural network method to solve the Helmholtz equation in the unbounded domain.*

Key words. Deep Learning, plane wave, deep neural network, loss, high frequency, Helmholtz equation.

1. Introduction

Scattering occurs when light, sound, or moving particles encounter inhomogeneities in their medium of propagation (e.g., the illuminated object has a curved or rough surface). As an illustration, a beam of light traveling through dilute milk appears pink when viewed from below, but light blue when viewed from the side and above. The study of scattering phenomena has close ties to engineering and technology, such as the use of tropospheric scattering for microwave or ultrashortwave in communication technology [22] and the investigation of the dynamical properties of atoms or electrons using scattering phenomena of various rays in the field of material science [32]. Due to the fact that scattering originates from the wave nature of matter [26, 33], its mathematical model is the standard wave equation or other equations derived from it. It is known, however, that the wave equation is a system of partial differential equations containing both time and space variables, which makes it more challenging to solve, especially when the boundary condition is complex, such as being unsmooth or unbounded. Thus, the Helmholtz equation, a simplified form of the time-independent wave equation obtained by using the separation of variables to simplify the analysis, has since become the landmark model for the study of scattering theory in its broadest sense. Moreover, if the Helmholtz equation is understood from the perspective of operator, the constant used to represent the wave frequency (or called wave number) can also be regarded as an eigenvalue, and the Helmholtz equation becomes an eigenvalue problem of the Laplace operator [13].

Received by the editors on April 17, 2023 and, accepted on September 7, 2023.
2000 *Mathematics Subject Classification.* 65L15, 34L16.

It is well known that when certain mathematical models are too complex to be solved analytically, it has become common subconscious to use computers for numerical simulations, as is the case with the wave equation and its simplified form, the Helmholtz equation. Notice that both, especially the latter, have a wide range of scientific and engineering applications, such as optics, acoustics, electricity, and quantum mechanics. For example, the cornerstone of non-relativistic quantum mechanics, Schrdinger's equation, is an extension of the Helmholtz equation, and a special case of the Helmholtz equation, the Laplace equation, also appears frequently in electrostatics. Thus, the ubiquitous application of these fundamental physical models in natural sciences, from satellite launches in space engineering or radar signal propagation in submarines to the design of cell phones or the acoustic detection of advanced materials, has driven the urgent need to design reliable and accurate numerical methods for them. This is also the purpose of this paper, namely to design reliable and accurate numerical methods for computing numerical solutions to the Helmholtz equation using computer technology.

However, not only is it not easy to simulate them numerically, but also very challenging. The main difficulty in solving the Helmholtz equation numerically comes from its non-positive definite structure, which causes a high degree of oscillation of the solution at large wave frequencies, leading to the so-called "pollution effect" [1], i.e., the approximate solution obtained in numerical calculations has only a very low accuracy. At the same time, we know that the scattering phenomenon of waves usually occurs in the unbounded region in practical physical and engineering applications. Consequently, for the Helmholtz equation over an unbounded region that is more applicable to real-world circumstances, the unbounded nature of the region poses additional obstacles to the development of effective and accurate numerical approaches. Therefore, this paper aims to address these two challenges simultaneously, i.e., designing reliable and accurate numerical methods for the Helmholtz equation with high frequency and located in the unbounded domain.

Indeed, we note that a considerable amount of work has been focused on dealing with these numerical challenges of the Helmholtz equation. The available numerical methods can be roughly divided into two main categories, namely, traditional mesh-based methods and novel meshless deep neural network (DNN) methods. In the following, we review these two categories of numerical methods for two different cases: bounded regions and unbounded regions, respectively.

For the case of bounded regions, the former traditional type of mesh-based methods for solving the Helmholtz equation includes the finite element method (FEM), Discontinuous Galerkin/ hybridizable discontinuous Galerkin/ weak Galerkin methods, and the Spectral method, etc. (see [1, 8, 25, 31, 37, 41] and reference therein), for dealing with the Helmholtz equation equipped with various boundary conditions in a finite bounded region. Due to the highly oscillatory character of the solution, higher-order polynomials or oscillatory non-polynomial basis [31, 45] are typically employed in these approaches to prevent pollution effects; however, the computational cost is significant due to the extra degrees of freedom. Using the latter type of methods, the recently prevalent DNN approach to solve the Helmholtz equation in bounded regions, has produced relatively little work to date. To name only a few that the author is aware of, existing approaches include the so-called Deep-Least Squares method (DLSM) developed in [6], the plane wave activation based neural network method (PWNN) in [42], and the ray-based DNN (RBDNN) method in our recent work [44], etc. Although the DNN method is still in its infancy in solving the Helmholtz equation, it has features that traditional methods do not have, such as its meshless nature that allows us to easily get away from designing adaptive meshes or applying specially designed spatial discretization methods, so it is very easy to implement. It can also more effectively and accurately approximate the exact solution of the Helmholtz equation, especially for the large frequency case, as evidenced by the numerical results obtained so far in [6, 44].

For the case of unbounded regions, all numerical methods that exist for solving the Helmholtz equation belong to the traditional type methods, i.e., the mesh-based methods such as the FEM, finite difference method, or Spectral method. Moreover, the unboundedness of regions requires special technical treatment, such as the need to reduce unbounded regions to bounded regions, which gives rise to the imperative requirement that the problem being reduced must be well-posed (existence, uniqueness and stability of the solution) and that the underlying solution must be as close as possible to the original solution in the truncated domain. Therefore, the development of efficient and robust domain truncation techniques for models over unbounded regions has become a long-standing research topic of great interest, of which successful techniques to date include the artificial boundary conditions (ABCs) [2, 20, 16, 15, 17, 19, 35, 34, 40], and the perfectly matched layer (PML) method developed in [5, 11, 4]. The idea of the ABCs method is to introduce an arbitrary boundary with artificial boundary conditions on it, such that the original problem is reduced to a boundary value problem in a bounded computational domain. The numerical approximation of the original problem can then be obtained by solving the reduced problem. The idea of the PML method is to surround the computational domain with a specially designed lossy medium that allows all waves propagating inside the computational domain to be attenuated. The major difference between the PML method and the ABCs method is that the PML method modify the governing equation accordingly so that any outgoing wave is perfectly transmitted from the domain to the layer regardless of the incident angle, while the ABCs method does not modify the equations. If the PML method is understood in the frequency domain, it can be simply interpreted as a complex coordinate stretch in the governing equation [11]. Since its inception, the PML method has been extensively investigated due to its superior accuracy and stability compared to the ABCs method. Many different PML absorption layers have been built [11, 40], and the PML method has even been incorporated into the toolkit of COMSOL, a commercial software for industrial computing.

Although the first type, mesh-based numerical methods, is well-established for the Helmholtz equation in the unbounded region, the second type, meshless DNN method, does not yet exist for this case. As described above, the DNN method has shown its superiority in dealing with bounded regions, i.e., it not only provides very good accuracy but also overcomes the "pollution effect" of using high-order polynomials for the high-frequency case. We also note that the DNN method has attracted extensive attention in recent years for many of the classical problems involved in scientific computing, especially the numerical solution of ordinary differential equations (ODE) or partial differential equations (PDE), cf. [30, 6, 3, 14, 18, 24, 23, 27, 28, 29, 36, 38, 43] and references therein. Therefore, a natural conjecture arises as to whether the DNN method can also be used for solving the Helmholtz equation in the unbounded region.

To address this conjecture, a new ray-based DNN-PML method referred to as RBDNN-PML, is proposed in this paper, whose main idea is to combine the ray-based DNN method for bounded regions proposed in our previous work [44] with the

PML method that deals with unbounded regions. We expect that such a combination can effectively and accurately solve the Helmholtz equation for high-frequency wave scattering over an unbounded domain. The construction of such a method is by no means an easy task because the steps of the method include not only the reformulation of the original equation but also the construction of the minimization objective function that allows the neural network to be trained. *This is a completely new approach and, to the author's knowledge, no method on DNNs has been applied to solve the high-frequency Helmholtz equations in unbounded regions.* Also, the authors believe that the method proposed in this paper is also quite adaptable and can be extended to solve other similar systems of ODEs or PDEs in unbounded regions, such as the wave equation, heat equation, or electromagnetic equations by using DNNs.

The rest of this article is organized as follows. In Section 3, we introduce the framework of the perfectly matched layer method and apply it for the Helmholtz scattering problem over the unbounded domain. The system in turn is transferred into a new form with easy boundary conditions in the finite bounded domain. In Section 4, we propose the meshless RBDNN-PML method for solving the new derived system. In Section 5, we present some numerical results to demonstrate the effectiveness and accuracy of our proposed method. Some concluding remarks and a discussion of future plans are given in Section 6.

2. Helmholtz scattering problem and PML method

2.1. Helmholtz scattering problem. The time-harmonic wave scattering problem reads as follows,

$$-\Delta u - k^2 u = f(\mathbf{x}), \qquad \text{in } \mathbb{R}^2, \tag{1a}$$

$$u = g(\mathbf{x}), \qquad \text{on } \Gamma_D, \tag{1b}$$

$$\sqrt{r}\left(\frac{\partial u}{\partial r} - \mathrm{i}ku\right) = 0, \qquad \text{as } r = |\boldsymbol{x}| \to \infty, \tag{1c}$$

where, u is the unknown complex wave function, $k > 0$ is the wave number, $f(\mathbf{x})$ is the known source term (in many work, f is simply set as zero), $\mathbb{R}^2$ is the two dimensional domain of real numbers $\mathbb{R}$, $\mathbf{x} \in \mathbb{R}^2$, i is the imaginary unit, D is a bounded domain in $\mathbb{R}^2$ with Lipschitz boundary Γ_D, $g \in H^{-\frac{1}{2}}(\Gamma_D)$ is determined by the incoming wave, and $\frac{\partial}{\partial r}$ means the partial derivative with r.

Note that the first boundary condition (1b) implies that the incident wave on the boundary of the illuminated object (i.e., Γ_D) is known, while the second condition (1c) means that at infinity, the wave has been completely attenuated to 0. For clarity, we depict the system (1a)-(1c) in the schematic diagram Fig. 1(a).

Remark 2.1. *For comparisons, we also give the Helmholtz equation over a finite bounded domain so that interested readers can clearly tell the significant differences between the two models. The Helmholtz equation in a finite bounded domain $\Omega \in \mathbb{R}^2$ reads as follows (cf.* [44, 6]*):*

$$-\Delta u - k^2 u = f(\mathbf{x}), \qquad \text{in } \Omega, \tag{2a}$$

$$u = g(\mathbf{x}), \qquad \text{on } \Gamma_D, \tag{2b}$$

$$\partial_{\mathbf{n}} u + \mathrm{i}ku = h(\mathbf{x}), \qquad \text{on } \Gamma_N, \tag{2c}$$

where $\partial\Omega$ denotes the boundary of Ω with $\Gamma_D \cup \Gamma_N = \partial\Omega$, and $\mathbf{n}$ denotes the outward unit normal vector field on Γ_N. The schematic diagram of the system (2a)-(2c) *is shown in Fig. 1(b).*

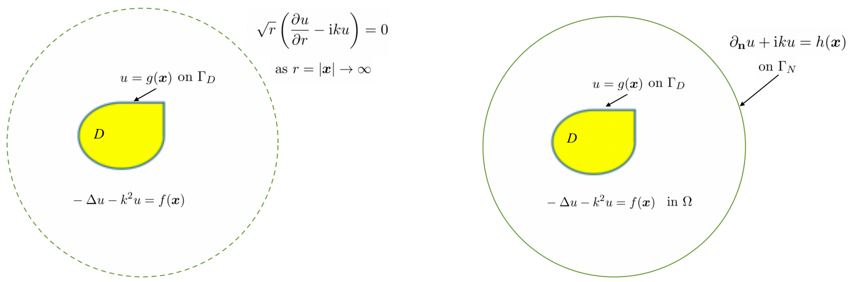

(a) Unbounded domain (b) Bounded domain

FIGURE 1. The comparison of the Helmholtz equation in the unbounded domain shown in (a) vs. the bounded domain shown in (b).

The PML method [5, 11, 4] can be viewed as a complex coordinate stretching of the original scattering problem (1a)–(1c), which usually has two versions, circular and uniaxial, and in the following we briefly describe each of them. The application of the PML method enables to transform the system in the unbounded region to the problem in the bounded region.

2.2. The circular PML method. We introduce two concentric circles, one large and one small, which are defined as $B_R = \{\boldsymbol{x} \in \mathbb{R}^2 : |\boldsymbol{x}| \le R\}$, and $B_\rho = \{\boldsymbol{x} \in \mathbb{R}^2 : |\boldsymbol{x}| \le \rho\}$, with $R < \rho$. The radius R is set big enough such that the domain D is contained in the interior of the circle B_R. We let $\Gamma_1 = \partial B_R$ and $\Gamma_2 = \partial B_\rho$. The PML interlayer located outside the small circle B_R and inside the large circle B_ρ is defined as Ω_{PML} with $\Omega_{PML} = \{\boldsymbol{x} \in \mathbb{R}^2 : R \le |\boldsymbol{x}| \le \rho\}$. The region that lies outside D and inside B_R is defined as $\Omega_1 = B_R \setminus D$. These symbols are depicted in the schematic diagram Fig. 2(a) along with the regions or boundaries they represent.

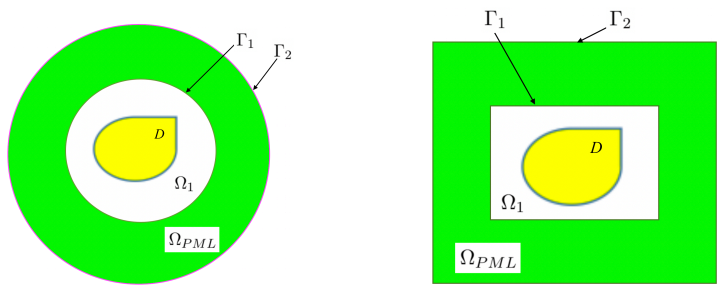

(a) Circular PML domain (b) Uniaxial PML domain

FIGURE 2. Schematic diagram of the circular PML domain shown in (a) and uniaxial PML domain shown in (b).

We define a complex function $\alpha(r)$ as the model medium property, such that

$$\alpha(r) = 1 + \mathrm{i}\sigma(r) \text{ with } \sigma \in C(\mathbb{R}), \sigma \ge 0, \text{and } \sigma = 0 \text{ for } r \le R.$$

In [9], a typical choice of $\sigma(r)$ is given as follows:

$$\sigma(r) = \sigma_0 \Big(\frac{r - R}{\rho - R}\Big)^m, \tag{3}$$

where σ_0 is a given constant in $\mathbb{R}$, and $m \geq 1$ is a given integer.

We define $\tilde{r}$ as the complex radius that is given as.

$$\tilde{r} = \tilde{r}(r) = \begin{cases} r, & \text{if } r \leq R, \\ \displaystyle\int_0^r \alpha(t)dt = r\beta(r), & \text{if } r \geq R. \end{cases}$$

Then, following the PML framework given in [12, 39], the Helmholtz equation (1a) can be reformulated to the following form:

$$\nabla \cdot (A\nabla \tilde{u}) + B\tilde{u} = 0 \text{ in } \mathbb{R}^2 \setminus \overline{B}_R, \tag{4}$$

where $A = HLH^T, B = k^2\alpha\beta$, and

$$L = \begin{pmatrix} \frac{\beta(r)}{\alpha(r)} & 0 \\ 0 & \frac{\alpha(r)}{\beta(r)} \end{pmatrix}, \quad H = \begin{pmatrix} \cos\theta & -\sin\theta \\ \sin\theta & \cos\theta \end{pmatrix}.$$

Thus, the reformulated Helmholtz equation with the circular PML reads as

$$\nabla \cdot (A\nabla \hat{u}) + B\hat{u} = 0, \quad \text{in } \Omega_{PML} \cup \Omega_1, \tag{5a}$$

$$\hat{u} = g, \quad \text{on } \Gamma_D, \tag{5b}$$

$$\hat{u} = 0, \quad \text{on } \Gamma_2. \tag{5c}$$

2.3. The Uniaxial PML method. We introduce two rectangles B_1, B_2 such that $D \subset B_1 \subset B_2$. The rectangle B_1 is defined as $B_1 = \{\boldsymbol{x} \in \mathbb{R}^2 : |x_1| \leq L_1/2, |x_2| \leq L_2/2\}$, and the rectangle B_2 is defined as $B_2 = \{\boldsymbol{x} \in \mathbb{R}^2 : |x_1| \leq L_1/2 + d_1, |x_2| \leq L_2/2 + d_2\}$. The rectangles are set big enough such that the domain D is contained in the interior of B_1. We let $\Gamma_1 = \partial B_1$, and $\Gamma_2 = \partial B_2$. These symbols are depicted in the schematic diagram Fig. 2(b) along with the regions or boundaries they represent.

We define two complex functions $\alpha_1(x_1)$ and $\alpha_2(x_2)$ as the model medium property. They read as $\alpha_1(x_1) = 1 + \mathrm{i}\sigma_1(x_1), \alpha_2(x_2) = 1 + \mathrm{i}\sigma_2(x_2)$, where

$$\sigma_j \in C(\mathbb{R}),\ \sigma_j \geq 0,\ \sigma_j(-t) = \sigma(t) \text{ and } \sigma = 0 \text{ for } r \leq L_j/2, j = 1, 2.$$

By [10], one can choose d_1, d_2 and $\sigma_j(t)$ such that

$$\frac{d_1}{L_1} = \frac{d_2}{L_2} = \chi, \tag{6}$$

and

$$\sigma_j(t) = \tilde{\sigma}_j \left(\frac{|t| - L_j/2}{d_j}\right)^m, \tag{7}$$

where χ is a given constant in $\mathbb{R}$, m is a given integer, and $\tilde{\sigma}_j = \dfrac{(m+1)\sigma}{d_j}$ for $j = 1, 2$.

We denote $\tilde{x}_j$ as the complex coordinate that reads as

$$\tilde{x}_j = \begin{cases} x_j, & \text{if } |x_j| \leq L_j/2, \\ \displaystyle\int_0^{x_j} \alpha(t)dt, & \text{if } |x_j| \geq L_j/2. \end{cases} \tag{8}$$

For the solution u of the Helmholtz scattering problem (1a)–(1c), let $\tilde{u} = \mathbb{E}(u|_{\Gamma_1})$ be an extension of $u|_{\Gamma_1}$. Then, following the PML method given in [10], one can derive that $\tilde{u}$ satisfies

$$\frac{\partial^2 \tilde{u}}{\partial \tilde{x}_1^2} + \frac{\partial^2 \tilde{u}}{\partial \tilde{x}_2^2} + k^2\tilde{u} = 0 \text{ in } \mathbb{R}^2 \setminus \overline{B}_1,$$

which yields the desired equation by applying the chain rule, as follows:

$$\nabla \cdot (A\nabla \tilde{u}) + B\tilde{u} = 0 \text{ in } \mathbb{R}^2 \setminus \overline{B}_1,$$

where $B = k^2\alpha_1(x_1)\alpha_2(x_2)$ and

$$A = \begin{pmatrix} \alpha_2(x_2)/\alpha_1(x_1) & \\ & \alpha_1(x_1)/\alpha_2(x_2) \end{pmatrix}.$$

Thus, the reformulated Helmholtz equation with the uniaxial PML reads as

$$\nabla \cdot (A\nabla \hat{u}) + B\hat{u} = 0, \quad \text{in } \Omega_{PML} \cup \Omega_1, \tag{9a}$$

$$\hat{u} = g, \quad \text{on } \Gamma_D, \tag{9b}$$

$$\hat{u} = 0, \quad \text{on } \Gamma_2. \tag{9c}$$

It can be seen that after the application of PML method, the original form of the equation is changed from (1a)-(1c) to (5a)-(5c) if using the circular PML and (9a)-(9c) if using the uniaxial PML. The Laplace operator of the original system is changed into a divergence-gradient operator with the variable coefficient A; the constant wave number part k^2u is also changed into variable coefficients $B\hat{u}$. Thus, if only looking at the form of the equation alone, one may have the illusion that the new system is actually more difficult to solve. But in fact this is not the case, as it can be seen that the complex boundary conditions of the original system become the homogenous Dirichlet type boundary conditions for the bounded regions. And this change is important, especially for the application of DNN methods to solve the system, because in our previous work [44], we have established the so-called ray-based DNN method for the Helmholtz equation in bounded regions. Hence, the PML method can be viewed as a bridge that allows us to extend the previously established methods [44] to unbounded regions. The application in PML gives us a great convenience because it is practically possible to obtain the DNN algorithm for the new model directly by changing the loss equation when building the neural network.

3. Methodology of RBDNN-PML for Helmholtz equation

In this section, we develop the RBDNN-PML methods (i.e., we firstly use the PML method to truncate the unbounded domain to a bounded domain, and then using the ray-based DNN method to solve the truncated problem) to solve the Helmholtz equation in the unbounded region. In the subsection 3.1, we give a brief introduction of the general DNN framework. In 3.2, the ray-based DNN method for the bounded domain Helmholtz problem is proposed. Since in Section 2, we have already transfer the unbounded domain problem to the problem in the bounded domain, thus in section 3.3, the RB-DNN method is applied to the new system by constructing the minimization objective function.

3.1. DNN method. A DNN is a sequential alternative composition of linear functions and nonlinear activation functions. A n-layer neutral network $\mathcal{N}^n$ can be defined as

- Input layer: $\mathcal{N}^0 = \boldsymbol{x}$,
- Hidden layers: $\mathcal{N}^l = \sigma_l(\mathbf{W}^l\mathcal{N}^{l-1} + \mathbf{b}^l)$, $l = 1, 2, \cdots, n-1$,
- Output layer: $\mathcal{N}^n = \mathbf{W}^n\mathcal{N}^{n-1} + \mathbf{b}^n$,

where σ denotes the activation function, $\mathbf{W}^l$ denote the weights and $\mathbf{b}^l$ denote the biases. The most common used types of activation functions include the sigmoid function $\sigma(t) = (1 + e^{-t})^{-1}$ and the rectified linear unit (ReLU) $\sigma(t) = \max(0, t)$.

For simplicity, we denote all the parameters in DNN by a parameter vector $\mathbf{\Theta}$, i.e.,

$$\mathbf{\Theta} = \{\mathbf{W^1}, \cdots, \mathbf{W^n}, \mathbf{b^1}, \mathbf{b^2}, \cdots, \mathbf{b^n}\}.$$

In Fig. 3, we sketch a simple fully connected DNN example with 3 hidden layers and 8 neurons in each hidden layer. The number m_l denotes the number of neurons in the l-th layer.

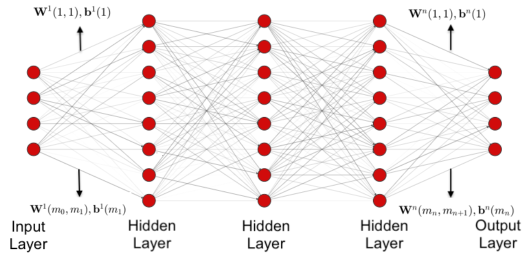

FIGURE 3. An example of a simple fully connected DNN.

3.2. Ray-based meshless DNN method. We consider the high frequency Helmholtz boundary value problem as follows

$$-\Delta u - k^2 u = f(\boldsymbol{x}) \text{ in } \Omega, \tag{10a}$$

$$u = u_D \text{ on } \partial\Omega. \tag{10b}$$

When adopting the DNN method, we train a neural network by minimizing some loss function. Define a space $P_{k,p}$ that is spanned by the plane wave functions with p different unit direction $\mathbf{d}_l \in R^{N-1}$ with $|\mathbf{d}_l| = 1$ and $l = 1, 2, \cdots, p$, such that

$$P_{k,p}(R^N) = \{u \in C^\infty(R^N) : u(\boldsymbol{x}) = \sum_{j=1}^{p} \alpha_l e^{\mathrm{i}k\boldsymbol{x}\cdot\mathbf{d}_l}\}. \tag{11}$$

Examples of such spaces are the so-called the ultra weak-variational formulation method [7], the plane-wave DG (discontinuous Galerkin) method [25].

Then, the meshless, Ray-based DNN method for solving (10a)–(10b) can be defined as

$$u_d(\boldsymbol{x}, \mathbf{\Theta}) = \sum_{j=1}^{p} e^{\mathrm{i}k\boldsymbol{x}\cdot\mathbf{d}_j} \mathcal{N}_j(\boldsymbol{x}, \mathbf{\Theta}), \tag{12}$$

where $\mathcal{N}_j(\boldsymbol{x}, \mathbf{\Theta}) = \mathcal{N}_j^{\mathrm{R}}(\boldsymbol{x}, \mathbf{\Theta}) + \mathrm{i}\mathcal{N}_j^{\mathrm{I}}(\boldsymbol{x}, \mathbf{\Theta})$ with $\mathcal{N}_j^{\mathrm{R}}(\boldsymbol{x}, \mathbf{\Theta})$ and $\mathcal{N}_j^{\mathrm{I}}(\boldsymbol{x}, \mathbf{\Theta})$ represent two different DNNs which are independent with each other.

The DNN in (12) is used to compute the solution of Helmholtz equations by minimizing the least squares of the Helmholtz equation's residual, which are given by the loss function as follows:

$$loss(\mathbf{\Theta}) = loss_{eq}(\mathbf{\Theta}) + \varrho loss_{bc}^{D}(\mathbf{\Theta}), \tag{13}$$

where ϱ denotes a penalty parameter and

$$loss_{eq}(\mathbf{\Theta}) = \sum_{m=1}^{N} |f(\boldsymbol{x}_m) - \Delta u_d(\boldsymbol{x}_m, \mathbf{\Theta}) - k^2 u_d(\boldsymbol{x}_m, \mathbf{\Theta})|^2, \tag{14a}$$

$$loss_{bc}^{D}(\mathbf{\Theta}) = \sum_{m=1}^{M_1} |u_D(\boldsymbol{x}_m) - u_d(\boldsymbol{x}_m, \mathbf{\Theta})|^2, \tag{14b}$$

with N, M_1 denote the number of choosing points in $\Omega, \partial\Omega$.

In practice, the integral of the above loss function is usually computed by a numerical way. A commonly-used approach in machine learning method is to use the Monte Carlo integration that is given below. For any v, the numerical integral of it reads as

$$\int_{\Omega} v(\boldsymbol{x})d\boldsymbol{x} = \frac{|\Omega|}{N}\sum_{i=1}^{N} v(\boldsymbol{x}_i), \tag{15}$$

where $|\Omega|$ is the volume of the domain Ω and $\{\boldsymbol{x}_i\}_{i=1}^N$ are the random points in Ω.

3.3. RBDNN-PML method. Based on the strategy of the RBDNN method ((12)-(14b)) constructed for the Helmholtz equation in bounded domain and the new system ((5a)–(5b) or (9a)–(9b)) after using the PML method, we propose a DNN method for the reformulated Helmholtz scattering problem with PML as

$$u(\boldsymbol{x}, \boldsymbol{\Theta}) = \begin{cases} u_1(\boldsymbol{x}, \boldsymbol{\Theta}_1) = \sum_{j=1}^{p} e^{\mathrm{i}k\boldsymbol{x}\cdot\mathbf{d}_j}\mathcal{N}_j(\boldsymbol{x}, \boldsymbol{\Theta}_1), & \boldsymbol{x} \in \Omega_1, \\ u_2(\boldsymbol{x}, \boldsymbol{\Theta}_2) = \mathcal{N}_{p+1}(\boldsymbol{x}, \boldsymbol{\Theta}_2), & \boldsymbol{x} \in \Omega_{PML}. \end{cases} \tag{16}$$

The DNN in (16) is used to compute the solution of PML problem by minimizing the following least squares of the residual,

$$loss(\boldsymbol{\Theta}) = loss_{eq}(\boldsymbol{\Theta}_1) + \varrho_1 loss_{in}^D(\boldsymbol{\Theta}_1) + loss_{pml}(\boldsymbol{\Theta}_2) + \varrho_2 loss_{out}^D(\boldsymbol{\Theta}_2) + \varrho_3 loss_{if}(\boldsymbol{\Theta}), \tag{17}$$

where $\varrho_i (i = 1, 2, 3)$ denote three penalty parameters and

$$\begin{aligned}
loss_{eq}(\boldsymbol{\Theta}_1) &= \sum_{m=1}^{N_1} |-\Delta u_1(\boldsymbol{x}_m, \boldsymbol{\Theta}_1) - k^2 u_1(\boldsymbol{x}_m, \boldsymbol{\Theta}_1)|^2, \\
loss_{in}^D(\boldsymbol{\Theta}_1) &= \sum_{m=1}^{M_1} |g(\boldsymbol{x}_m) - u_1(\boldsymbol{x}_m, \boldsymbol{\Theta}_1)|^2, \\
loss_{pml}(\boldsymbol{\Theta}_2) &= \sum_{m=1}^{N_2} |\nabla\cdot(A\nabla u_2(\boldsymbol{x}_m, \boldsymbol{\Theta}_2)) + Bu_2(\boldsymbol{x}_m, \boldsymbol{\Theta}_2)|^2, \\
loss_{out}^D(\boldsymbol{\Theta}_1) &= \sum_{m=1}^{M_3} |u_2(\boldsymbol{x}_m, \boldsymbol{\Theta}_2)|^2, \\
loss_{if}(\boldsymbol{\Theta}) &= \sum_{m=1}^{M_2} |u_1(\boldsymbol{x}_m, \boldsymbol{\Theta}_1) - u_2(\boldsymbol{x}_m, \boldsymbol{\Theta}_2)|^2.
\end{aligned}$$

with N_1, N_2 denote the number of choosing points in Ω_1, Ω_{PML} and M_1, M_2, M_3 denote the number of choosing points in $\partial D, \Gamma_1, \Gamma_\rho$.

4. Numerical example

In this section, we implement numerical examples to verify the effectiveness of the proposed meshless DNN method in solving the Helmholtz equation with high wave numbers and unbounded domain.

Example 1. In the first numerical example, we set the scattering region D be a unit circle with radius $a = 1$, and suppose the exact solution is known, that is $u = H_0^{(1)}(kr)$ where $H_0^{(1)}$ denotes the zeroth-order Hankel function of the first kind.

We take $R = 0.3, \rho = 1, \sigma = 30$. We set $\mathcal{N}^{\mathrm{R}}(\boldsymbol{x}), \mathcal{N}^{\mathrm{I}}(\boldsymbol{x})$ to be 4 hidden layers with 80 neurons in each hidden layer for $k = 100$, and 10 hidden layers with 100 neurons in each hidden layer for $k = 500$. In the learning process, we choose the points in each epoch to be 1000. The maximum errors on the domain $\Omega_1 = \{\boldsymbol{x} \in \mathbb{R}^2 : |\boldsymbol{x}| \in [0.3, 0.8]\}$ are shown in Table 1 for each case and various epochs. We see that as the number of epochs increases, the errors of real and imaginary parts both decrease to the scale of 10^{-6}, which shows that the numerical solution of our proposed DNN method converges very well to the exact solution. The profiles of the computed solution using 5000 epochs for $k = 500$ are shown in Fig. 4. These results show that even when k is large, the DNN method can also solve the Helmholtz scattering problem well.

TABLE 1. Example 1: maximum error with various epochs for $k = 100$ and $k = 500$.

k	No. of points	epoch	Re-Error	Im-Error
100	2500*2500	1000	1.4e-1	1.4e-1
		5000	2.4e-2	2.4e-2
		7000	8.8e-3	8.9e-3
		10000	4.4e-3	4.4e-3
500	5000*5000	1000	3.6e-1	3.5e-1
		5000	4.3e-2	4.4e-2
		8000	8.8e-3	8.7e-3
		10000	7.7e-3	7.8e-3

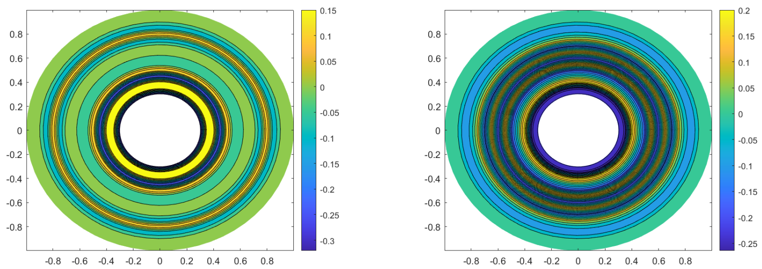

(a) The real part (b) The imaginary part

FIGURE 4. Example 1 with $k = 500$: (a) the real part, and (b) imaginary part of the computed solution.

Example 2. In the second numerical example, we set the scattering domain D to be rectangular with $D = [-0.4, 0.4] \times [-0.4, 0.4]$. Similar to the previous example, we also set the exact solution as $u = H_0^{(1)}(kr)$. We take $L_1 = L_2 = 1.4, d_1 = d_2 = 0.3$. We set $\mathcal{N}^{\mathrm{R}}(\boldsymbol{x}), \mathcal{N}^{\mathrm{I}}(\boldsymbol{x})$ to be 6 hidden layers with 40 neurons in each hidden

TABLE 2. Example 2: maximum error with various epochs for $k = 500$ and $k = 3000$.

k	No. of points	epoch	Re-Error	Im-Error
500	500*500	500	7.2e-1	7.7e-1
		3000	5.7e-1	6.0e-1
		6000	2.2e-2	2.4e-2
		20000	1.1e-3	1.2e-3
3000	3000*3000	1000	4.7e-1	4.9e-1
		4000	8.4e-2	8.4e-2
		7000	3.8e-2	3.7e-2
		30000	1.4e-3	1.3e-3

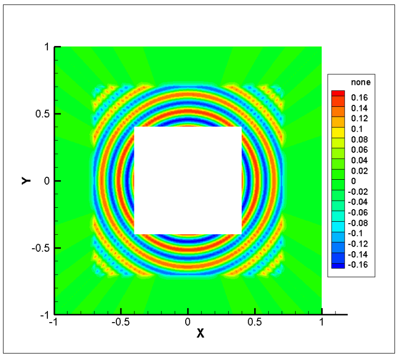

(a) real part

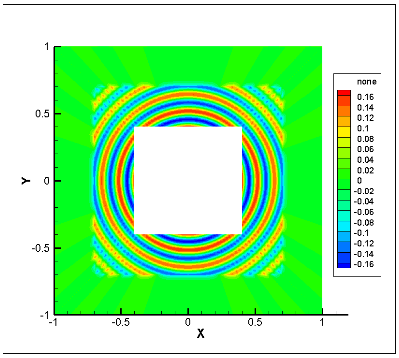

(b) imaginary part

FIGURE 5. Example 2 with $k = 3000$: (a) the real part, and (b) imaginary part of the computed solution.

layer for $k = 500$, and 10 hidden layers with 80 neurons in each hidden layer for $k = 3000$. In the learning process, we choose the points in each epoch to be 1000. The maximum errors on the domain $\Omega_1 = \{\boldsymbol{x} \in \mathbb{R}^2 : |\boldsymbol{x}| \in [-0.7, 0.7]^2 \setminus [-0.4, 0.4]^2\}$ are shown in Table 2 for each case and various epochs. These accuracy results show that for the square region in this example, our proposed DNN method also solves the Helmholtz scattering problem well for very large wave frequency numbers k. In Fig. 5, we also the profiles of the solution u that is computed using 10000 epochs for $k = 3000$.

Example 3. In the third numerical example, we consider the scattering domain D is a circle and the incoming wave is a plane wave, propagating along the x-axis. Suppose the incoming wave can be written in polar coordinate as

$$u_{inc} = -e^{\mathrm{i}kx} = -\sum_{n=-\infty}^{\infty} \mathrm{i}^{-n} J_n(k\rho) e^{\mathrm{i}n\theta}.$$

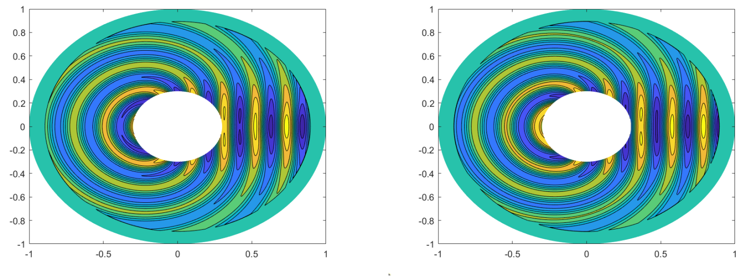

(a) real part (b) imaginary part

FIGURE 6. Example 3 with $k = 30$: (a) the real part, and (b) imaginary part of the computed solution.

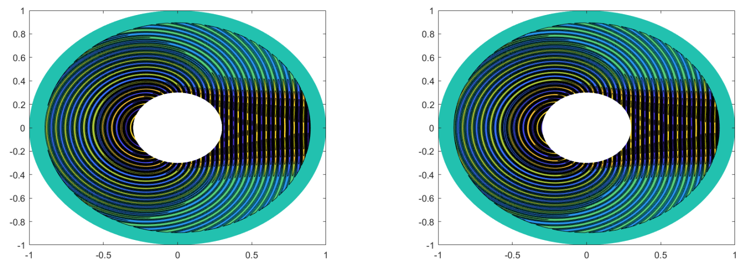

(a) real part (b) imaginary part

FIGURE 7. Example 3 with $k = 100$: (a) the real part, and (b) imaginary part of the computed solution.

The exact solution for the scattering of such a wave from a circular disk is given by the series

$$U_{ex}(\rho,\phi) = -\sum_{n=0}^{\infty} \mathrm{i}^n J_n(kR)\frac{H_n^{(1)}(k\rho)}{H_n^{(1)}(ka)}e^{\mathrm{i}n\theta}. \tag{18}$$

We set $\mathcal{N}^{\mathrm{R}}(\boldsymbol{x}), \mathcal{N}^{\mathrm{I}}(\boldsymbol{x})$ to be 8 hidden layers with 100 neurons in each hidden layer, $\Omega_1 = \{\boldsymbol{x} \in \mathbb{R}^2 : |\boldsymbol{x}| \in [0.3, 0.8]\}$, $\Omega_{PML} = \{\boldsymbol{x} \in \mathbb{R}^2 : |\boldsymbol{x}| \in [0.8, 1]\}$. In Fig. 6 and Fig. 7 , we plot the profiles of the solution u that is computed using 10000 epochs for $k = 30$ and $k = 100$, respectively. Both numerical results show the wave propagation pattern, especially for high frequencies $k = 100$, and the numerical results are very accurate and robust to obtain the signature propagation morphology of scattered waves.

5. Concluding remarks

In this paper, we propose a novel, efficient, and robust numerical method for solving the high-frequency Helmholtz scattering problem in the unbounded region. The proposed method is based on the combination of the PML method and the ray-based DNN method. The numerical results demonstrate the effectiveness of the proposed method in providing a highly accurate approximation of the exact solution. As the approach provided in this study is sufficiently generic, it is expected that comparable methods can be derived in future research to solve other systems in unbounded regions, such as the wave equation, heat equation, or electromagnetic equations by using the DNN method. Some discussions on those topics are given below.

• Extension to high dimension: The numerical methods and numerical experiments in this paper are actually for 2D (two-dimensional) space, while 3D (three-dimensional) space is more than just adding a spatial variable the algorithm and computational consumption will need to be changed accordingly or even completely different. The extension/generalization of the PML method as well as designing a DNN method for the Helmholtz equation in the 3D domain while ensuring feasible computational cost is by no means an easy task, which is the first plan of the author.

• Extension to the wave equation: In the author's previous work [44] and this article, all numerical algorithms are designed for solving the Helmholtz equation, which belongs to the so-called ODE system, i.e., all derivatives are only for spatial variables. Indeed, most mathematical systems describing the laws of nature are systems of PDEs, i.e., the derivatives include not only space but also time, e.g., the wave equations, the fluid dynamics systems, etc. One of the current hot research topics in the computational community has been the application of machine learning methods in an attempt to find more accurate and stable mathematical methods [14, 21]. Therefore, one of the author's further research plans is to extend the ray-based approach designed in this paper to the wave equations, and the combination of DNN and PML techniques designed in this paper to the wave equations over unbounded regions. This method is sufficiently adaptable and therefore it is highly possible to establish a framework for the design of efficient numerical methods for the wave equations without losing specialty but in a uniform manner.

• DNN method for coupled nonlinear type models: Most of the physical models that had been widely used and studied in the natural science are so-called coupled nonlinear models, where multiple variables are coupled together in a nonlinear manner, such as the Navier-Stokes equations in fluid dynamics, which are nonlinear due to the presence of advection terms and the system also contains two variables, the velocity field and the pressure; and the Maxwell equations describing the electromagnetic field, which consist of four coupled equations. It should be noted that the DNN method constructed in this paper is only for a simple linear system containing only one variable, then how to construct a DNN algorithm for a nonlinear system with multiple variables is also one of the plans that the author is very interested in and ready to implement.

Acknowledgment

The author would like to thank Professor Feng Gu of the Department of Computer Science at the City University of New York for his constructive comments and valuable suggestions, and the author's parents for their support.

References

[1] I. Babuska and S. Sauter. Is the pollution effect of the fem avoidable for the helmholtz equation considering high wave numbers?. *SIAM J. Numer. Anal.*, 34(6):2392–2423, 1997.

[2] W. Bao and H. Han. High-order local artificial boundary conditions for problems in unbounded domains. *Compu. Meth. Appl. Mech. Eng.*, 188:455–471, 2000.

[3] C. Beck, M. Hutzenthaler, A. Jentzen, and B. Kuckuck. An overview on deep learning-based approximation methods for partial differential equations. *arXiv:2012.12348*, 2020.

[4] J. P. Berenger. A perfectly matched layer for the absorption of electromagnetic waves. *J. Comp. Phys.*, 114(2):185–200, 1994.

[5] J. P. Berenger. Three-dimensional perfectly matched layer for the absorption of electromagnetic waves. *J. Comp. Phys.*, 127(2):363–379, 1996.

[6] W. Cai, X. Li, and L. Liu. A phase shift deep neural network for high frequency approximation and wave problems. *SIAM J. Sci. Comput.*, 42(5):A3285–A3312, 2020.

[7] O. Cessenat and B. Despres. Application of an ultra weak variational formulation of elliptic pdes to the two-dimensional helmholtz problem. *SIAM J. Numer. Anal.*, 35(1):255–299, 1998.

[8] H. Chen, P. Lu, and X. Xu. A hybridizable discontinuous galerkin method for the helmholtz equation with high wave number. *SIAM J. Numer. Anal.*, 51(4):2166–2188, 2013.

[9] Z. Chen and X. Liu. An adaptive perfectly matched layer technique for time-harmonic scattering problems. *SIAM J. Numer. Anal.*, 43(2):645–671, 2005.

[10] Z. Chen and X. Wu. An adaptive uniaxial perfectly matched layer method for time-harmonic scattering problems. *Numer. Math. Theor. Meth. Appl*, 1:113–137, 2008.

[11] W. Chew and W. Weedon. A 3d perfectly matched medium from modified Maxwell's equations with stretched coordinates. *Micro. and opt. tech. lett.*, 7(13):599–604, 1994.

[12] F. Collino and P. Monk. The perfectly matched layer in curvilinear coordinates. *SIAM J. Sci. Comput.*, 19(6):2061–2090, 1998.

[13] G. de Mey. Calculation of eigenvalues of the helmholtz equation by an integral equation. *Inter. J. for Num. Meth. Eng.*, 10(1):59–66, 1976.

[14] W. E and B. Yu. The deep ritz method: a deep learning-based numerical algorithm for solving variational problems. *Commun. Math. Stat.*, 6(1):1–12, 2018.

[15] B. Engquist and A. Majda. Absorbing boundary conditions for the numerical simulation of waves. *Math. Comp.*, 31:629–651, 1977.

[16] D. Gilbarg and N.S. Trudinger. Elliptic partial differential equations. *Springer-Verlag, Berlin*, 1977.

[17] C. I. Goldstein. A finite element method for solving helmholtz type equations in waveguides and other unbounded domains. *Math. Comp.*, 39:309–324, 1982.

[18] I. Gühring, G. Kutyniok, and P. Petersen. Error bounds for approximations with deep relu neural networks in $w^{s,p}$ norms. *Anal. Appl.*, 18(05):803–859, 2020.

[19] T. Hagstrom. A new construction of perfectly matched layers for hyperbolic systems with. In *Mathematical and Numerical Aspects of Wave Propagation WAVES 2003: Proceedings of the Sixth International Conference on Mathematical and Numerical Aspects of Wave Propagation Held at Jyvèaskylèa, Finland, 30 June-4 July 2003*, page 125. Springer Science & Business Media, 2003.

[20] T. Hagstrom and H. B. Keller. Exact boundary conditions at an artificial boundary for partial differential equations in cylinders. *SIAM J. Math. Anal.*, 17(2):322–341, 1986.

[21] H Han, A. Jentzen, and W. E. Solving high-dimensional partial differential equations using deep learning. *PNAS: Proceedings of the National Academy of Sciences of the United States of America*, 115:8505–8510, 2018.

[22] K. M. Harb, S. S. I. Mitu, M. Ullah, and H. Attia. Nonuniform scattering of microwave radiation due to layered dusa storm: Theory and experiment. *IEEE Canad. J. Elec. Comp. Eng.*, 44(3):384–389, 2021.

[23] J. He, L. Li, J. Xu, and C. Zheng. Relu deep neural networks and linear finite elements. *J. Comput. Math.*, 38(3):502–527, 2020.

[24] J. He and J. Xu. Mgnet: A unified framework of multigrid and convolutional neural network. *Sci. China Math.*, 62(7):1331–1354, 2019.

[25] R. Hiptmair, A. Moiola, and I. Perugia. Plane wave discontinuous galerkin methods for the 2d helmholtz equation: analysis of the p-version. *SIAM J. Numer. Anal.*, 49(1):264–284, 2011.

[26] J. S. Hubert and E. S. Palencia. The helmholtz equation in unbounded domains. *In: Hubert, J.S., Palencia, E.S. (eds) Vibration and Coupling of Continuous Systems. Springer, Berlin, Heidelberg.*, 1989.

[27] G. Karniadakis, I. Kevrekidis, L. Lu, P. Perdikaris, S. Wang, and L. Yang. Physics-informed machine learning. *Nat. Rev. Phys.*, 3(6):422–440, 2021.

[28] R. Khodayi-Mehr and M. Zavlanos. Varnet: Variational neural networks for the solution of partial differential equations. In *Learning for Dynamics and Control*, pages 298–307. PMLR, 2020.

[29] L. Lu, X. Meng, Z. Mao, and G. Karniadakis. Deepxde: A deep learning library for solving differential equations. *SIAM. Rev.*, 63(1):208–228, 2021.

[30] J. Meade, J. Andrew, and A. Fernandez. The numerical solution of linear ordinary differential equations by feedforward neural networks. *Math. Comp. Modelling*, 19(12):1–25, 1994.

[31] M. Melenk and S. Sauter. Wavenumber explicit convergence analysis for galerkin discretizations of the helmholtz equation. *SIAM J. Numer. Anal.*, 49(3):1210–1243, 2011.

[32] Y. B. Melnichenko and G. D. Wignall. Small-angle neutron scattering in materials science: Recent practical applications. *J. Appl. Phys.*, 102:021101, 2007.

[33] I. Newton. A letter of mr. isaac newton containing his new theory about light and colours. *Phil. Trans.*, 6:3087, 1665.

[34] P. G. Petropoulos. Reflectionless sponge layers as absorbing boundary conditions for the numerical solution of maxwell equations in rectangular, cylindrical, and spherical coordinates. *SIAM J. Appl. Math.*, 60(3):1037–1058, 2000.

[35] P. G. Petropoulos. Reflectionless sponge layers for the numerical solution of maxwell's equations in cylindrical and spherical coordinates. *Appl. Num. Math.*, 33(1):517–524, 2000.

[36] E. Samaniego, C. Anitescu, S. Goswami, V. Nguyen-Thanh, H. Guo, K. Hamdia, X. Zhuang, and T. Rabczuk. An energy approach to the solution of partial differential equations in computational mechanics via machine learning: Concepts, implementation and applications. *Comput. Methods Appl. Mech. Eng.*, 362:112790, 2020.

[37] J. Shen and L.-L. Wang. Spectral approximation of the helmholtz equation with high wave numbers. *SIAM J. Numer. Anal.*, 43(2):623–644, 2005.

[38] J. Sirignano and K. Spiliopoulos. Dgm: A deep learning algorithm for solving partial differential equations. *J. Comput. Phys.*, 375:1339–1364, 2018.

[39] F. Teixeira and W. Chew. Complex space approach to perfectly matched layers: a review and some new developments. *Inter. J. Num. Mod.: Elec. Net., Dev. Fields*, 13(5):441–455, 2000.

[40] E. Turkel and A. Yefet. Absorbing PML boundary layers for wave-like equations. *Appl. Numer. Math.*, 27(4):533, 1998.

[41] J. Wang and Z. Zhang. A hybridizable weak galerkin method for the helmholtz equation with large wave number: hp analysis. *Int. J. Numer. Anal. Model.*, 14(4–5):744–761, 2017.

[42] Z. Wang, T. Cui, and X. Xiang. A neural network with plane wave activation for helmholtz equation. *arXiv:2012.13870*, 2020.

[43] Z. Wang and Z. Zhang. A mesh-free method for interface problems using the deep learning approach. *J. Comput. Phys.*, 400:108963, 2020.

[44] A. L. Yang and F. Gu. A mesh-less, ray-based deep neural network method for the helmholtz equation with high frequency. *Int. J. Numer. Anal. Mod.*, 19:587–601, 2022.

[45] L. Zhu and H. Wu. Preasymptotic error analysis of CIP-FEM and FEM for Helmholtz equation with high wave number. Part II: hp version. *SIAM J. Numer. Anal.*, 51(3):1828–1852, 2013.

† Dutchfork High School, Irmo, SC, USA
E-mail: yangandy2006@gmail.com.